Journal of Insights in Basic and Applied Sciences
مجلة رؤى في العلوم الأساسية والتطبيقية
ISSN: 3106-1737
Volume 2, Issue 3, 2026, Pages: 41-49
Journal homepage: https://jibas.com.ly/index.php/jibas/en

Structural, Microstructural, and Superconducting Properties of Si-substituted YBa2 Cu3 O7- δ Ceramics

Najah Ibrahem Elharari [1 *], Sanaa Masod Abdulqader [2]
[1] Higher Institute of Medical Sciences and Technology/ Abu salim, Tripoli, Libya
[2] Department of Physics Science, Faculty of Education/ Kikla, University of Gharyan, Libya

الخصائص التركيبية والمجهرية وخصائص الموصلية الفائقة لسيراميك *YBa2 Cu3 O7- δ* المستبدل بالسيليكون

نجاح ابراهيم الحراري [1*]، سناء مسعود عبد القادر [2]
[1] المعهد العالي للعلوم والتقنيات الطبية / أبو سليم، طرابلس، ليبيا
[2] قسم علوم الفيزياء، كلية التربية/ ككلة، جامعة غريان، ليبيا

*Corresponding author: 1 najahalharari92@gmail.com, 2 sanaamasod1985@gmail.com

Received: May 19, 2026	Accepted: June 25, 2026	Published: July 08, 2026

Abstract:
This study investigates the effect of Silicon (Si) substitution on the microstructure and superconducting properties of the Y Ba2(Cu1-x Si x)3 O7-δ high-temperature superconductor, with composition ranging from x = 0.00 to x = 0.03. Samples were synthesized using the conventional solid-state reaction method. The morphological and microstructural characteristics were examined using Scanning Electron Microscopy (SEM). The results indicate that while the pure sample (x = 0.00) exhibits rectangular block grains aligned in preferred directions, the Si-substituted samples show a tendency toward grain size reduction, with an average grain size found to be less than 2 \mu m for all compositions. Furthermore, the microstructure of the substituted samples reveals a higher degree of irregularity, flaky grain shapes, and increased porosity at higher Si concentrations, which significantly reduces the connectivity between grains. Although the study highlights morphological changes, these structural modifications are critical for understanding the superconducting behavior, as they directly impact the critical current density and overall material performance. The findings suggest that Si substitution influences the grain growth mechanism and density of the Y Ba2(Cu1-x Si x)3 O7-δ system, emphasizing the importance of optimizing processing parameters to maintain superconducting performance in polycrystalline ceramics.

Keywords: Y Ba2(Cu1-x Si x)3 O7-δ, Silicon substitution, High-temperature superconductor, Microstructure, Scanning Electron Microscopy.

الملخص
تتناول هذه الدراسة تأثير استبدال السيليكون (Si) على البنية المجهرية وخصائص الموصلية الفائقة للمركب YBa2 Cu3 O7-δ ذي درجة الحرارة العالية، بنسب استبدال تتراوح من x = 0.00 إلى x = 0.03. تم تحضير العينات باستخدام طريقة تفاعل الحالة الصلبة التقليدية، وجرى فحص الخصائص المورفولوجية والمجهرية باستخدام المجهر الإلكتروني الماسح (SEM). تشير النتائج إلى أنه بينما تُظهر العينة النقية (x = 0.00) حبيبات مستطيلة الشكل متراصة في اتجاهات مفضلة، فإن العينات المستبدلة بالسيليكون تميل إلى انخفاض حجم الحبيبات، حيث وُجد أن متوسط الحجم أقل من 2 ميكرومتر لجميع التراكيب. علاوة على ذلك، كشفت البنية المجهرية للعينات المستبدلة عن درجة أعلى من عدم الانتظام في أشكال الحبيبات، مع زيادة في الفجوات والمسامية عند تركيزات السيليكون العالية، مما قلل من الترابط بين الحبيبات بشكل ملحوظ. وعلى

الرغم من أن الدراسة تسلط الضوء على التغيرات المورفولوجية، فإن هذه التعديلات الهيكلية تعد حاسمة لفهم سلوك الموصلية الفائقة، حيث تؤثر بشكل مباشر على كثافة التيار الحرج والأداء العام للمادة. تشير النتائج إلى أن استبدال السيليكون يؤثر على آلية نمو الحبيبات وكثافة نظام YBa2 Cu3 O7-δ ، مما يؤكد أهمية تحسين معايير المعالجة للحفاظ على أداء الموصلية الفائقة في السيراميك متعدد البلورات.

الكلمات المفتاحية YBa2 Cu3 O7-δ: ، استبدال السيليكون، موصل فائق ذو درجة حرارة عالية، البنية المجهرية، المجهر الإلكتروني الماسح.

Introduction

Superconductivity is a quantum phenomenon characterized by the transition of a material into a state of zero electrical resistance and the expulsion of magnetic fields (the Meissner effect) when cooled below a specific critical temperature (T_c) (Tinkham, 2004). Since the discovery of high-temperature superconductivity in cuprates, these materials have remained at the forefront of condensed matter physics due to their immense potential in technological applications, ranging from power transmission to quantum computing (Bednorz & Müller, 1986).

Superconductors are generally classified based on their magnetic response into Type I, which exhibit a sharp transition to the superconducting state, and Type II, which allow partial magnetic field penetration through flux vortices (Bardeen et al., 1957). Furthermore, they are categorized by their critical temperatures: low-temperature superconductors (LTS), which typically require liquid helium cooling, and high-temperature superconductors (HTS), which can operate at liquid nitrogen temperatures (77 K) (Schilling et al., 1993).

The discovery of Y $Ba_2(Cu_{1-x}$ Si $_x)_3$ $O_{7-\delta}$ (YBCO) in 1987 marked a paradigm shift, as it was the first material to demonstrate superconductivity above 77 K (Wu et al., 1987). Prior to this milestone, the highest known T_c was approximately 23 K in Nb_3 Ge, necessitating costly liquid helium refrigeration (Kirkup, 1988). The ability to use liquid nitrogen—which is significantly cheaper and more abundant—opened new avenues for large-scale industrial applications (Ginsberg, 1989).

Despite this progress, the widespread adoption of polycrystalline YBCO is constrained by two primary challenges. First, while YBCO single crystals exhibit high critical current densities (J_c), polycrystalline samples often suffer from weak-link behavior at grain boundaries, which severely limits their current-carrying capacity (Dimos et al., 1988). Second, the material's bulk properties are highly sensitive to its processing history, including calcination temperatures, sintering cycles, and oxygen annealing, all of which dictate the final microstructure, phase purity, and density (Goodenough & Manthiram, 1990).

To address these limitations, chemical substitution (doping) in the Y-Ba-Cu-O system has emerged as a vital strategy to manipulate lattice defects, optimize grain growth, and enhance superconducting characteristics (Yao et al., 2000). Silicon (Si) substitution, in particular, offers a unique opportunity to study the effects of atomic size mismatch and valence states on the Cu-O planes, which are the fundamental pathways for charge carriers (Ekin et al., 1989). This study aims to investigate the influence of Si incorporation on the microstructural evolution and superconducting performance of Y $Ba_2(Cu_{1-x}$ Si $_x)_3$ $O_{7-\delta}$ providing insight into how compositional tuning can mitigate grain connectivity issues and improve the viability of these ceramics for advanced applications.

The selection of Silicon (Si) as a dopant in the YBa_2 Cu_3 $O_{7-\delta}$ system is motivated by its unique ionic characteristics compared to copper. Given the significantly smaller ionic radius of Si^{4+} compared to the Cu^{2+}/Cu^{3+} sites, the substitution is expected to introduce localized lattice strain and structural distortions within the Cu-O planes. These modifications in the crystalline lattice are hypothesized to alter the electronic environment and the density of states near the Fermi level, thereby influencing the charge carrier dynamics and the superconducting coherence within the system. Investigating these effects provides critical insight into the relationship between structural perturbations and the suppression or enhancement of superconducting properties.

Fundamental Properties of Superconductors

Superconductivity is a distinct quantum state of matter, fundamentally defined by two macroscopic phenomena: the total disappearance of electrical resistivity (p= 0) and the manifestation of perfect diamagnetism, commonly known as the Meissner-Ochsenfeld effect (Tinkham, 2004). This transition occurs abruptly at a material-specific critical temperature (Tc). According to the Bardeen-Cooper-Schrieffer (BCS) theory, superconductivity emerges from the attractive interaction between electrons mediated by lattice vibrations, known as phonons. This interaction leads to the formation of "Cooper pairs," which behave as bosons and condense into a single coherent quantum state, enabling charge transport through the crystal lattice without energy dissipation due to scattering (Bardeen et al., 1957).

Perfect diamagnetism represents the thermodynamic stability of the superconducting state in an external magnetic field. Unlike a perfect conductor, which merely maintains existing currents, a superconductor actively expels magnetic flux lines from its interior (Abd-Shukor, 2004). This expulsion is achieved by the generation of persistent surface currents that create an internal magnetic field exactly equal and opposite to the applied external field, resulting in a net magnetic induction of zero (B = 0) inside the bulk (Meissner, 1933). This unique property facilitates remarkable applications such as magnetic levitation and high-field superconducting magnets.

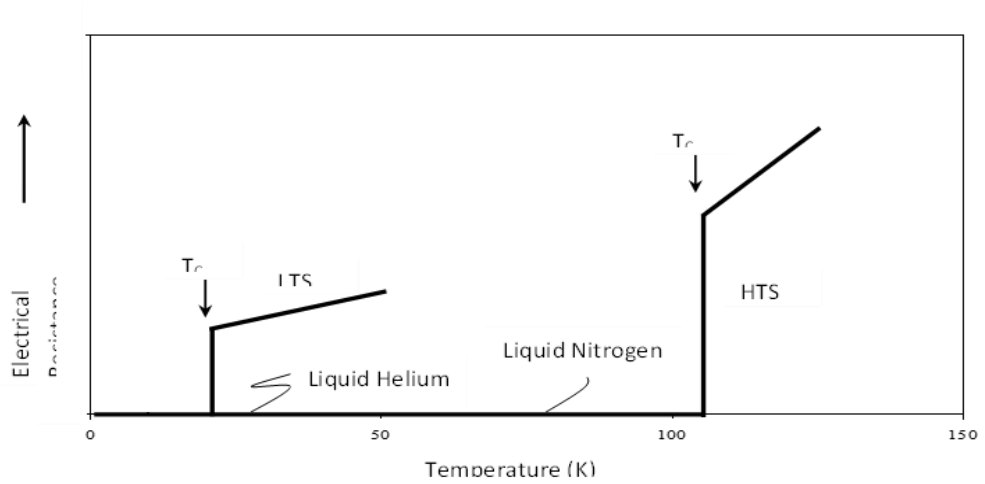

Figure 1. Zero electrical resistance (R=0 K)

Literature Review: Elemental Substitution In Ybco

The physical and superconducting properties of Y $Ba_2(Cu_{1-x}$ Si $_x)_3$ $O_{7-\delta}$ (YBCO) are highly sensitive to chemical modifications at the copper sites. Numerous studies have employed elemental substitution to tailor the microstructure and investigate the mechanism of superconductivity. For instance, Takuya and Yoshida (2002) explored the effects of Praseodymium (Pr) doping, demonstrating through Scanning Electron Microscopy (SEM) that Pr influences the nucleation and growth rates of YBCO grains, thereby altering the critical current density (J_c).

In parallel, the investigation of transition metal substitution has provided significant insights into structural modulation. Jardim and Gama (1989) reported that Manganese (Mn) substitution promotes the formation of densely packed, plate-like grain morphologies, which are often preferred for improved grain boundary connectivity. Conversely, investigations into the incorporation of Antimony (Sb) by Akhtar et al. (2000) revealed that the resulting microstructure is critically dependent on thermal processing parameters, such as the cooling rate (furnace-cooled vs. quenched), which dictates the oxygen stoichiometry and defect distribution. Research on Tin (Sn) substitution by Zheng and Zhang (2002) highlighted the fine balance required during synthesis; while low doping levels maintain the desired crystalline homogeneity, higher concentrations ($x > 0.3$) trigger the precipitation of deleterious secondary phases at the grain boundaries, which act as insulating barriers to supercurrent flow.

Crystal Structure And Microstructural Characterization

The high-temperature superconductivity in YBCO is intrinsically linked to its layered orthorhombic structure, which consists of alternating layers of Cu-O planes and Cu-O chains, separated by *Y* and *Ba* atoms (Goodenough & Manthiram, 1990). The Cu-O planes are identified as the primary pathways for superconductive charge transport, and any distortion to this lattice—through either oxygen deficiency or elemental substitution—directly influences the superconducting performance (Kirkup, 1988).

To investigate the morphology of the synthesized ceramics, microstructural analysis was performed using a Philips XL 30 Scanning Electron Microscope. High-resolution SEM micrographs were recorded at an accelerating voltage of 15 kV. To prepare the samples for analysis, the fractured internal surfaces were coated with a conductive gold layer via vacuum evaporation, which minimizes charging effects and enhances the contrast at the grain boundaries. This technique is essential for evaluating key microstructural features, such as average grain size, grain orientation, and the presence of porosity, all of which are statistically correlated with the material's connectivity and its ability to sustain a high critical current density.

4. Synthesis And Stoichiometric Calculations

The samples were synthesized using the conventional solid-state reaction method. The starting precursors (Y_2 O_3, BaO, CuO, and SiO_2) were stoichiometrically weighed and ground to ensure homogeneity before thermal treatment. The chemical reaction is described by the following general equation:

Calculation of Sample preparation of YBa_2 $(Cu_{1-x}$ $Si_x)_3$ O_7

The reaction equation given by:

$$\tfrac{1}{2}\,(Y_2O_3) + 2(BaO) + (3 \times (1-x))\,CuO + (3 \times x)\,SiO \rightarrow YBa_2\,(Cu_{1-x}\,Si_x)_3\,O_7$$

The atomic weight of the main elements of the system:

Y = 88.90585
Ba = 137.327
Cu = 63.546
O = 15.9994
Si = 28.0855

a) When (x = 0.00)

Formula weight oxides of $YBa_2 (Cu_{1-0.00} Si_{0.00})_3 O_{7:}$

½ (Y_2O_3) = ½ (2 × 88.90585 + 3 × 15.9994) = 112.90495

2(BaO) = 2(137.327 + 15.9994) = 306.6528

3CuO =3CuO = 3× (63.546 + 15.9994) = 238.6362

The total Formula weight of $YBa_2 (Cu_{1-0.04} Si_{0.04})_3 O_7$:

Total = 112.90495 + 306.6528 +238.6362 = 658.19395

To prepare 3 g of sample, each oxides powder can be calculated as:

Weight of ½ (Y_2O_3) = $\frac{112.90495}{658.19395} \times 3 = 0.5146$ g

Weight of 2(BaO) = $\frac{306.6528}{658.19395} \times 3 = 1.3977$ g

Weight of 3CuO = $\frac{238.6362}{658.19395} \times 3 = 1.0877$ g

The total of oxides powder:

Total = 0.5146 + 1.3977 + 1.0877 = 3 g

b) When (x = 0.01)

Formula weight oxides of $YBa_2 (Cu_{1-0.01} Si_{0.01})_3 O_{7:}$

½ (Y_2O_3) = ½ (2 × 88.90585 + 3 × 15.9994) = 112.90495

2(BaO) = 2(137.327 + 15.9994) = 306.6528

(3 × (1 – 0.01)) CuO = (3 × 0.99) CuO = 2.97 (63.546 + 15.9994) = 236.249838

(3 × 0.99) SiO = 2.97(28.0855 + 15.9994) = 1.322547

The total Formula weight of $YBa_2 (Cu_{1-0.01} Si_{0.01})_3 O_7$:

Total = 112.90495 + 306.6528 + 236.249838+1.322547 = 657.130135

To prepare 3 g of sample, each oxides powder can be calculated as:

Weight of ½ (Y_2O_3) = $\frac{112.90495}{657.1301} \times 3 = 0.5154$g

Weight of 2(BaO) = $\frac{306.6528}{657.1301} \times 3 = 1.4$g

Weight of 2.88 CuO = $\frac{236.249838}{657.1301} \times 3 = 1.0786$ g

Weight of 0.12 SiO= $\frac{1.322547}{657.1301} \times 3 = 0.06$ g

The total of oxides powder:

Total of all weight = 3 g

c) when (x = 0.02)

Formula weight oxides of $YBa_2 (Cu_{1-0.02} Si_{0.02})_3 O_7$:

½ (Y_2O_3) = ½ (2 × 88.90585 + 3 × 15.9994) = 112.90495

2 (BaO) = 2 (137.327 + 15.9994) = 306.6528

(3 × (1 – 0.02)) CuO = (3 × 0.98) CuO = 2.94 × 79.5454= 223.863476

(3 × 0.98) SiO = 2.94 (28.0855 + 15.9994) = 2.645094

The total Formula weight of $YBa_2 (Cu_{1-0.02} Si_{0.02})_3 O_7$:

Total = 112.90495 + 306.6528 +223.863476 +2.645094 = 656.06632

To prepare 3 g of sample, each oxides powder can be calculated as:

Weight of ½ (Y_2O_3) = $\frac{112.90495}{656.06632} \times 3 = 0.5163$g

Weight of 2(BaO) = $\frac{306.6528}{656.06632} \times 3 = 1.4022$ g

Weight of 2.85 CuO = $\frac{223.863476}{656.06632} \times 3 = 1.0694$ g

Weight of 0.15 SiO = $\frac{2.645094}{656.06632} \times 3 = 0.0121$g

The total of oxides powder:

Total of all weight = 3 g

d) when (x = 0.03)

Formula weight oxides of $YBa_2 (Cu_{1-0.03} Si_{0.03})_3 O_7$:

½ (Y_2O_3) = ½ (2 × 88.90585 + 3 × 15.9994) = 112.90495

2 (BaO) = 2 (137.327 + 15.9994) = 306.6528

(3 × (1 – 0.03)) CuO = (3 × 0.97) CuO = 2.91 × 79.5454 = 231.477114

(3 × 0.97) SiO = 2.91 (28.0855 + 15.9994) = 3.967641

The total Formula weight of $YBa_2 (Cu_{1-0.03} Si_{0.03})_3 O_7$:

Total = 112.90495 + 306.6528 +231.477114 +3.967641 = 655.002505

To prepare 3 g of sample, each oxides powder can be calculated as:

Weight of ½ (Y_2O_3) = $\frac{112.90495}{655.002505} \times 3 = 0.5171$ g

Weight of 2(BaO) = $\frac{306.6528}{655.002505} \times 3 = 1.4045$g

Weight of 2.79 CuO = $\frac{231.477114}{655.002505} \times 3 = 1.0602$g

Weight of 0.21 SiO= $\frac{3.967641}{655.002505} \times 3 = 0.0182$ g

The total of oxides powder:

Total of all weight = 3 g

Microstructural Analysis

The morphological characteristics of the Y $Ba_2(Cu_{1-x}\ Si_{\ x})_3\ O_{7-\delta}$ ($0.00 \leq x \leq 0.03$) ceramic samples were investigated using a Philips XL 30 Scanning Electron Microscope (SEM) at an accelerating voltage of 15 kV. Representative micrographs for each composition are presented in Figures 1 through 4. The average grain sizes were determined using the linear intercept method from multiple SEM images, and the results are summarized in Table 1.

Table 1. Average grain size of Y $Ba_2(Cu_{1-x}\ Si_{\ x})_3\ O_{7-\delta}$ samples

Composition (x)	Average Grain Size (μm)
0.00	1.8
0.01	2.0
0.02	1.9
0.03	1.4

The SEM micrograph of the pure YBCO sample (x=0.00) reveals a well-defined morphology characterized by rectangular block-like grains aligned in specific preferred orientations, consistent with the orthorhombic structure of high-quality YBCO ceramics (Kirkup, 1988). Although the pure sample exhibits relative structural integrity, some isolated intergranular gaps and voids are observed, which are typical in solid-state sintered ceramics.

Upon the introduction of Silicon as a dopant, a distinct morphological evolution is observed. All Si-substituted samples exhibit a transition towards flaky, plate-like grain shapes, which become increasingly irregular and randomly distributed, lacking the preferential alignment observed in the pure sample. As the Silicon concentration increases from x=0.01 to x=0.03, a general downward trend in the average grain size is evident, reaching a minimum of 1.4μm at x=0.03.

The observed reduction in grain size and the increase in intergranular porosity at higher substitution levels suggest that Silicon ions (Si^{4+}) effectively act as grain-growth inhibitors. This phenomenon is likely attributed to the lattice strain induced by the ionic size mismatch between Si and the host Cu sites, which hinders grain boundary migration during the sintering process. Furthermore, the increase in gaps and voids at higher Si concentrations indicates a degradation of the intergranular connectivity (the "weak-link" effect), which is fundamentally detrimental to the critical current density (J_c) of the material (Dimos et al., 1988). These microstructural observations confirm that while low-level substitution may slightly modify grain growth, higher concentrations significantly disrupt the continuous superconducting path within the polycrystalline matrix.

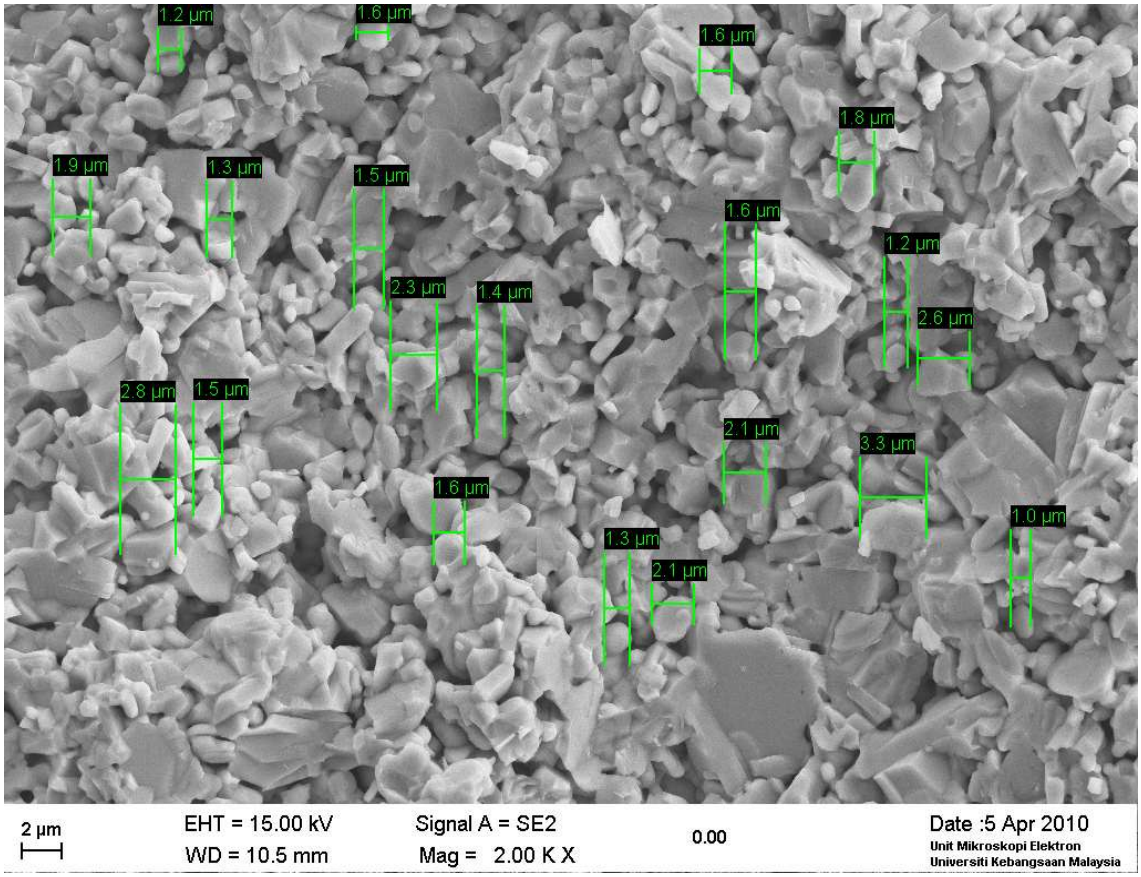

Figure (1) SEM images of YBa_2 $(Cu_{3-x}\,Si_x)$ O_{7-x} with x = 0.00

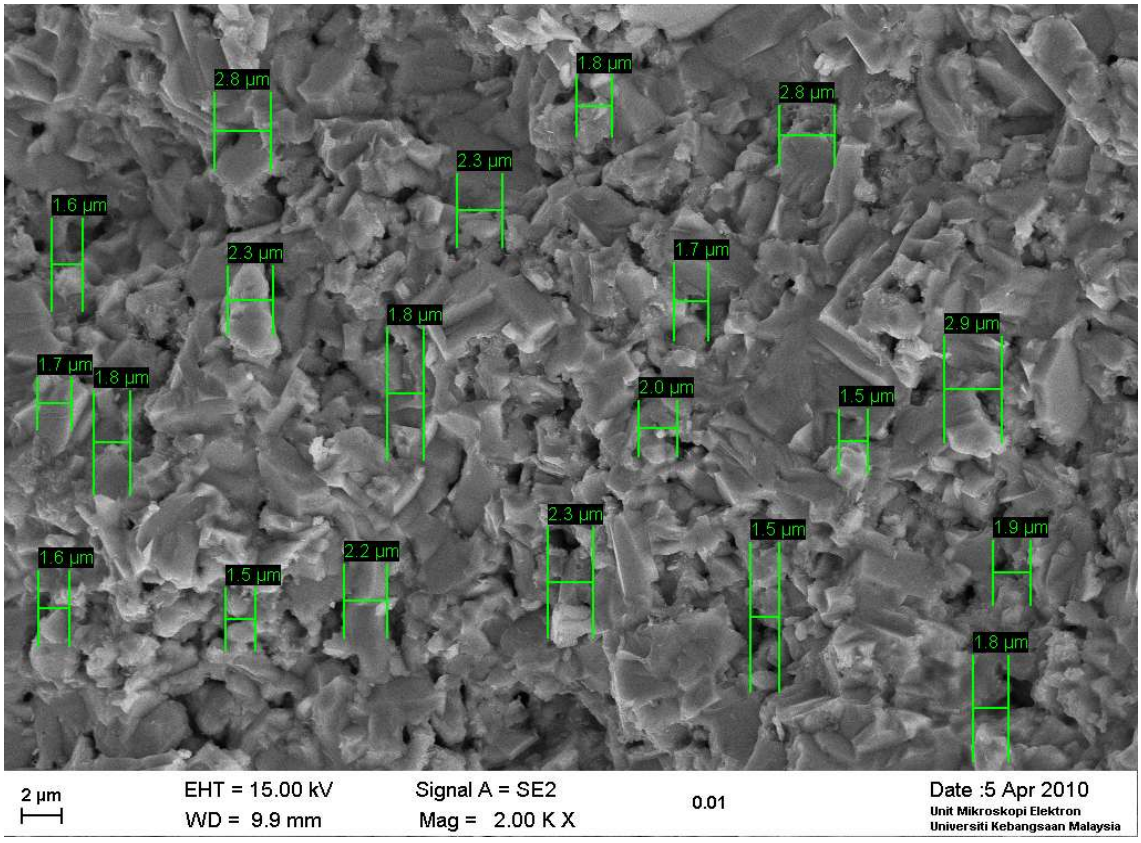

Figure (2) SEM images of YBa_2 $(Cu_{3-x}\,Si_x)$ O_{7-x} with x = 0.0

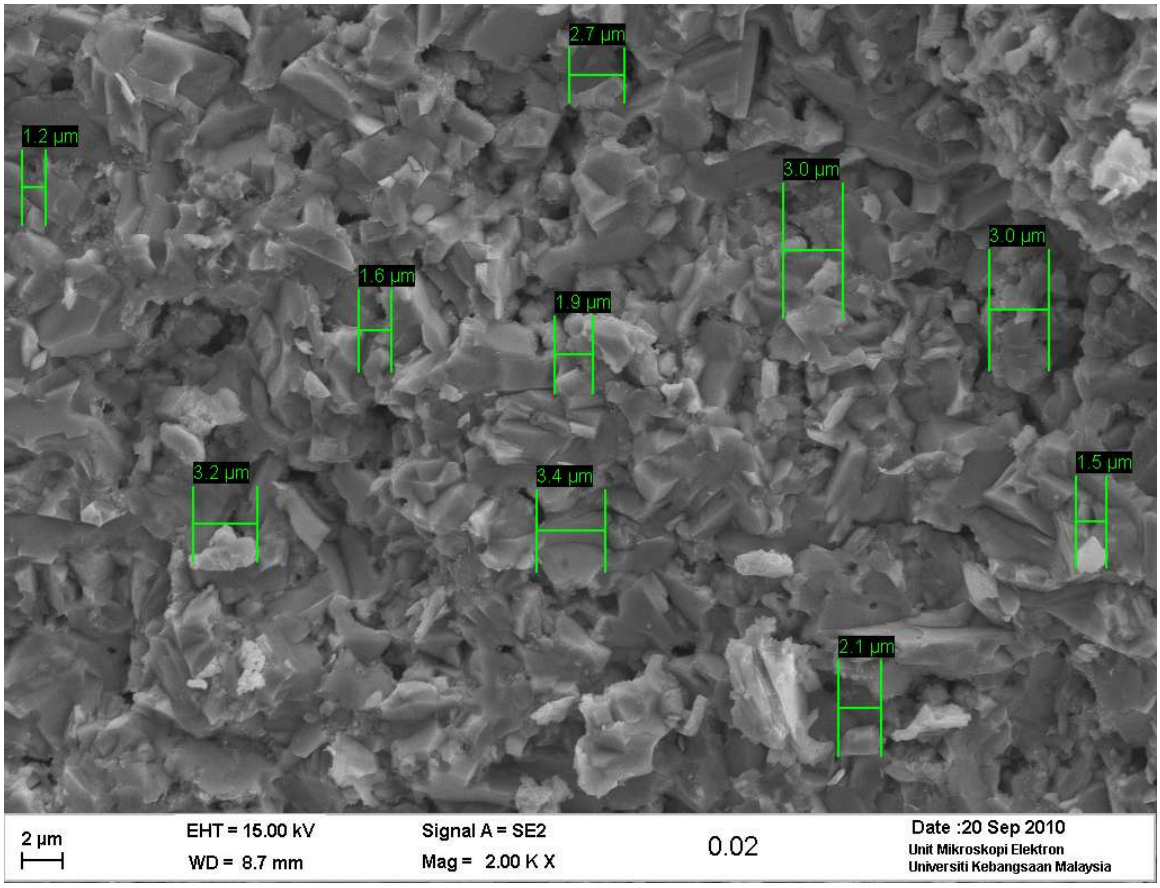

Figure (3) SEM images of $YBa_2 (Cu_{3-x} Si_x) O_{7-x}$ with x = 0.02

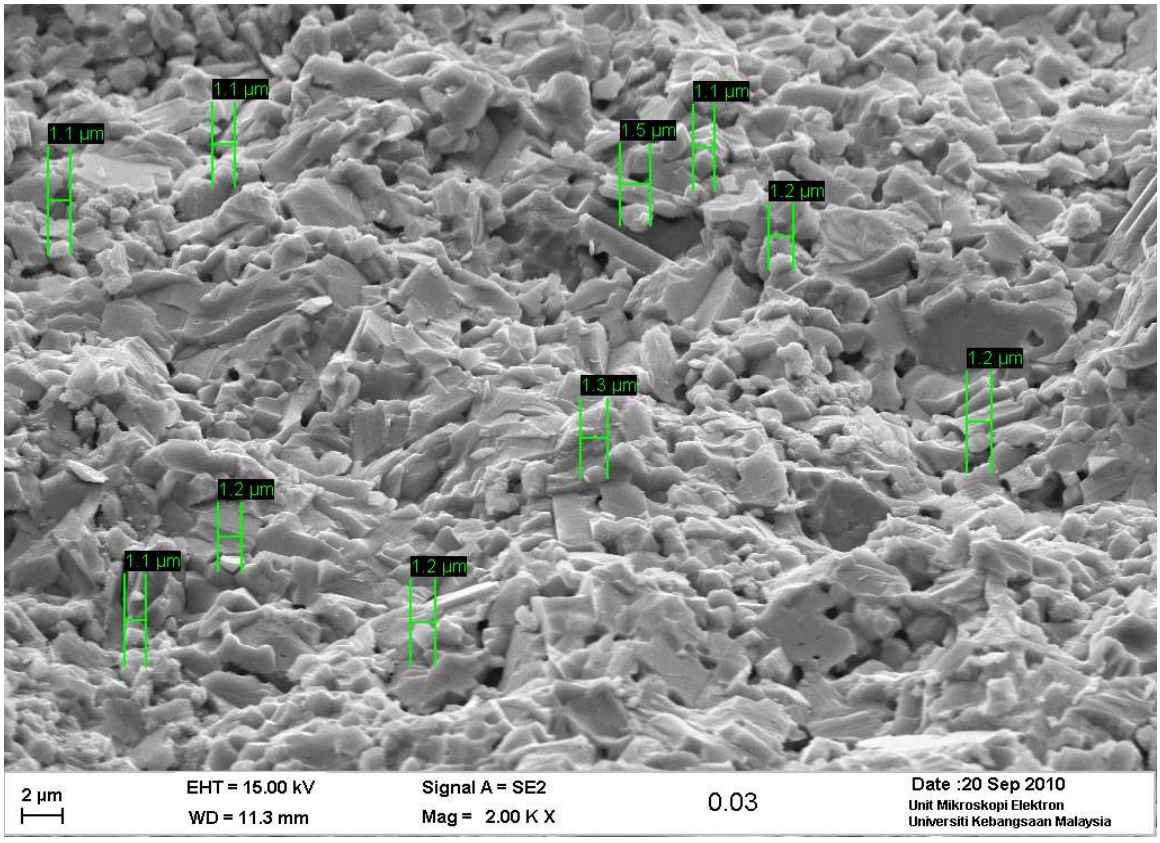

Figure (4) SEM images of $YBa_2 (Cu_{3-x} Si_x) O_{7-x}$ with x = 0.0

RESULTS

The structural integrity and morphological evolution of the $Y\,Ba_2(Cu_{1-x}\,Si_x)_3\,O_{7-\delta}$ ($0.00 \leq x \leq 0.03$) ceramic system were systematically evaluated. The experimental findings confirm that the substitution of Silicon for Copper does not inhibit the formation of the base YBCO phase; however, it induces significant variations in the microstructural architecture, which are critical for understanding the physical properties of these polycrystalline superconductors.

- ***Microstructural Morphological Evolution***

The surface morphology of the samples, captured via Scanning Electron Microscopy (SEM) and presented in Figures 1–4, reveals a clear transition in grain growth mechanisms upon Si doping. The undoped sample (x=0.00) displays a characteristic high-density structure composed of well-defined, rectangular, and block-shaped grains. These grains exhibit a distinct parallel alignment, which is an indicator of favorable crystal growth conditions during the conventional solid-state sintering process.

Upon introducing Silicon into the lattice, the morphology undergoes a marked transformation. As seen in the micrographs of the x=0.01 to x=0.03 samples, the grains deviate from the stoichiometric rectangular geometry, shifting toward irregular, flaky, and plate-like configurations. This transition suggests that Silicon ions create localized lattice distortions, effectively disrupting the long-range order of grain boundary migration. Notably, the grain size distribution shows a non-monotonic trend: it reaches a slight peak at x=0.01 (2.0 μm) before experiencing a sustained decrease, concluding at 1.4 μm for the x=0.03 composition. This statistical reduction in grain size is a direct consequence of the dopant-induced inhibition of grain boundary mobility, which limits the development of larger grains during the sintering phase.

- ***Analysis of Porosity and Intergranular Connectivity***

The integrity of grain boundaries is a dominant factor in determining the current-carrying capacity of ceramic superconductors. The SEM analysis demonstrates a clear correlation between Silicon concentration and the proliferation of intergranular voids. While the x=0.00 sample maintains a relatively compact structure with minimal intergranular spacing, the substituted samples exhibit a significant increase in the volume fraction of pores.

In samples with $x \geq 0.02$, these voids become pervasive, physically segmenting the superconducting grains. The emergence of these gaps acts as a series of insulating barriers, which significantly compromises the "weak-link" behavior of the polycrystalline ceramic. The transition from a dense, well-connected network to a porous, fragmented microstructure suggests that higher levels of Silicon substitution ($x > 0.02$) negatively impact the percolation of the superconducting current. Consequently, these structural defects are expected to create significant bottlenecks for charge carrier flow across the grain boundaries, which provides a morphological basis for the expected reduction in the global critical current density (J_c) of the material. The increase in porosity, coupled with the change in grain shape, confirms that while Silicon is successfully incorporated, its presence is a primary factor in the microstructural degradation of the YBCO matrix.

Conclusion

This study successfully synthesized and characterized the $Y\,Ba_2(Cu_{1-x}\,Si_x)_3\,O_{7-\delta}$ ($0.00 \leq x \leq 0.03$) ceramic system to investigate the impact of Silicon substitution on the microstructure and physical properties of the YBCO matrix. The microstructural analysis, conducted via SEM, confirms that while Silicon incorporation is achievable using the conventional solid-state reaction method, it induces significant morphological transformations.

The key findings are as follows:

1. **Morphological Transition:** Silicon acts as a grain growth inhibitor, causing the grain morphology to transition from well-ordered, rectangular, and block-like structures in the pure YBCO sample to smaller, irregular, and flaky grain shapes in the Si-substituted samples.
2. **Grain Size Reduction:** A systematic reduction in the average grain size was observed as the Silicon content increased, reaching a minimum average size of 1.4 μm at the maximum substitution level (x=0.03).
3. **Connectivity Deterioration:** High concentrations of Silicon ($x \geq 0.02$) promote the proliferation of intergranular voids and porosity. These structural defects function as insulating barriers, which disrupt the integrity of the superconducting current paths and significantly weaken the intergranular connectivity (the "weak-link" effect).

In conclusion, while Silicon substitution allows for the study of doping effects in the Y-Ba-Cu-O system, the resulting microstructural degradation—specifically the increased porosity and reduced grain connectivity—suggests that excessive Silicon content is detrimental to the overall superconducting performance. Future research should focus on optimizing the sintering thermal profile or utilizing secondary processing techniques to mitigate the porosity observed at higher substitution levels. This study provides a foundational understanding of the microstructural-property relationship in Si-doped YBCO, which is essential for the design and improvement of high-temperature superconducting ceramics for practical technological applications.

References

[1] Abd-Shukor, R. (2004). *Introduction to superconductivity in metals, alloys & cuprates*. Penerbit Universiti Pendidikan Sultan Idris.

[2] Akhtar, M. J., Shaheen, R., Haque, M. N., Bashir, J., & Akhetr, J. I. (2000). Synthesis and characterization of $YBa_2(Cu_{3-x}\ Sb_x)\ O_{7-\delta}$ high-temperature superconductors. *Superconductor Science and Technology*, *13*(11), 1612–1616.
[3] Bardeen, J., Cooper, L. N., & Schrieffer, J. R. (1957). Theory of superconductivity. *Physical Review*, *108*(5), 1175–1204.
[4] Bednorz, J. G., & Müller, K. A. (1986). Possible high T_c superconductivity in the Ba-La-Cu-O system. *Zeitschrift für Physik B Condensed Matter*, *64*(2), 189–193.
[5] Dimos, D., Chaudhari, P., Mannhart, J., & LeGoues, F. K. (1988). Orientation dependence of grain-boundary critical currents in $YBa_2\ Cu_3\ O_{7-\delta}$ bicrystals. *Physical Review Letters*, *61*(2), 219–222.
[6] Goodenough, J. B., & Manthiram, A. (1990). Oxide superconductors. *Journal of Solid State Chemistry*, *88*(1), 115–139.
[7] Jardim, R. F., & Gama, S. (1989). Enhanced grain growth in $YBa_2\ (Cu_{1-x}\ Mn_x)_3\ O_{7-\delta}$ compounds. *Physica C: Superconductivity*, *159*(3), 306–310.
[8] Kirkup, L. (1988). Resistance measurements as a function of temperature on the high-T_c superconductor $YBa_2\ Cu_3\ O_{7-x}$. *European Journal of Physics*, *9*(1), 1–4.
[9] Takuya, H., & Yoshida, K. (2002). Effect of Pr doping on the critical current density in $YBa_2\ Cu_3\ O_{7-\delta}$ prepared by the solid-state reaction method. *Journal of Applied Physics*, *91*(9), 5988–5992.
[10] Tinkham, M. (2004). Introduction to superconductivity (2nd ed.). Dover Publications.
[11] Wu, M. K., Ashburn, J. R., Torng, C. J., Hor, P. H., Meng, R. L., Gao, L., Huang, Z. J., Wang, Y. Q., & Chu, C. W. (1987). Superconductivity at 93 K in a new mixed-phase Y-Ba-Cu-O compound system at ambient pressure. Physical Review Letters, 58(9), 908–910.
[12] Zheng, G., & Zhang, J. (2002). The effect of tin substitution on ferroelectric ordering of Cu-O in YBCO oxides. Superconductor *Science and Technology*, *15*(10), 1398–1402